



Contents lists available at ScienceDirect

Bioorganic & Medicinal Chemistry Letters

journal homepage: www.elsevier.com/locate/bmcl

Targeting prostate cancer with compounds possessing dual activity as androgen receptor antagonists and HDAC6 inhibitors

Pradeep S. Jadhavar^a, Sreekanth A. Ramachandran^a, Eduardo Riquelme^b, Ashu Gupta^a, Kevin P. Quinn^c, Devleena Shivakumar^d, Soumya Ray^d, Dnyaneshwar Zende^a, Anjan K. Nayak^a, Sandeep K. Miglani^a, Balaji D. Sathe^a, Mohd. Raja^a, Olivia Farias^b, Ivan Alfaro^b, Sebastián Belmar^b, Javier Guerrero^b, Sebastián Bernales^c, Sarvajit Chakravarty^c, David T. Hung^c, Jeffrey N. Lindquist^{c,*}, Roopa Rai^{c,*}

^a Integral BioSciences Pvt. Ltd, C-64, Hosiery Complex Phase II Extension, Noida, Uttar Pradesh 201306, India

^b Fundación Ciencia y Vida, Avenida Zañartu 1482, Ñuñoa, Santiago 7780272, Chile

^c Medivation, 525 Market Street, 36th Floor, San Francisco, CA 94105, USA

^d Schrodinger, Inc., Portland, OR, USA

ARTICLE INFO

Article history:

Received 6 September 2016

Revised 22 September 2016

Accepted 23 September 2016

Available online xxxxx

Keywords:

Prostate cancer

Enzalutamide

HDAC6 inhibitor

Androgen receptor (AR) antagonist

Induced fit docking (IFD)

ABSTRACT

While enzalutamide and abiraterone are approved for treatment of metastatic castration-resistant prostate cancer (mCRPC), approximately 20–40% of patients have no response to these agents. It has been stipulated that the lack of response and the development of secondary resistance to these drugs may be due to the presence of AR splice variants. HDAC6 has a role in regulating the androgen receptor (AR) by modulating heat shock protein 90 (Hsp90) acetylation, which controls the nuclear localization and activation of the AR in androgen-dependent and independent scenarios. With dual-acting AR–HDAC6 inhibitors it should be possible to target patients who don't respond to enzalutamide. Herein, we describe the design, synthesis and biological evaluation of dual-acting compounds which target AR and are also specific towards HDAC6. Our efforts led to compound **10** which was found to have potent dual activity (HDAC6 IC₅₀ = 0.0356 μM and AR binding IC₅₀ = <0.03 μM). Compound **10** was further evaluated for antagonist and other cell-based activities, in vitro stability and pharmacokinetics.

© 2016 Elsevier Ltd. All rights reserved.

It is widely recognized that chemotherapy drugs are most effective when given in combination. The rationale for combination therapy is to harness disparate mechanisms, thereby reducing the likelihood of resistance. Deriving from the same principles, it is possible to have a single molecule with dual activity. Cabozantinib is a small molecule tyrosine kinase inhibitor of cMet and VEGFR2; this dual activity has culminated in US FDA approvals for medullary thyroid cancer and advanced renal cell carcinoma and it is currently being tested in the clinic for various other cancers, including prostate cancer (PC).¹ At the research level, a recent Letter describes the synthesis and evaluation of dual-acting estrogen receptor (ER) and histone deacetylase (HDAC) inhibitors (HDACi).^{2,3} These ER–HDAC inhibitors combined ERα antagonist activity with potent HDAC inhibitor activity, resulting in better anti-tumor efficacy in ERα positive breast cancer cells in vitro when compared to the approved drug Tamoxifen.

HDACs modulate histone acetylation, which controls gene expression. HDAC inhibitors have been studied and tested in cancer treatment with numerous agents approved and others undergoing clinical trials.^{4,5} HDAC6 has been implicated in the pathogenesis and treatment of cancer⁶ and its role in regulating the androgen receptor (AR) by modulating heat shock protein 90 (Hsp90) acetylation has also been studied.^{7,8} Hsp90 acetylation controls the stability, nuclear localization and activation of the AR in androgen-dependent and independent scenarios. Inhibition of HDAC6 therefore provides an opportunity to target castration resistant prostate cancer.^{6–9}

Enzalutamide has proven to be clinically beneficial in metastatic castration-resistant prostate cancer (mCRPC).^{10–12} While enzalutamide and abiraterone¹³ are approved for treatment of mCRPC, approximately 20–40% of patients have no response to these agents. Moreover, it has been stipulated that the lack of response and the development of secondary resistance to these drugs may be due to the presence of AR splice variants.¹⁴ Meanwhile, the clinical evaluation of HDAC inhibitors as monotherapy for prostate cancer has not been promising. However using a

* Corresponding authors.

E-mail addresses: jeffrey.lindquist@medivation.com (J.N. Lindquist), roopa.raihotmail.com (R. Rai).

combination of an HDAC inhibitor with antiandrogens, a synergistic increase in cytotoxicity has been demonstrated in a number of hormone-sensitive and -resistant preclinical models.¹⁵ In such scenarios, dual-acting AR–HDAC6 inhibitors may be of value. The idea of using AR binding as a means of directing HDACi to prostate tumors has been explored, where AR binding is suggested as a homing device.³ These authors reported using cyanonilutamide as the AR binding element in their designs of dual AR–HDACi.³ Herein, we describe our efforts to make dual-acting compounds which target AR and are also specific towards HDAC6, using enzalutamide as the AR binding element. During the preparation of our manuscript, a similar hybrid molecule generated from enzalutamide and HDAC inhibitor such as Vorinostat was reported to inhibit viability of enzalutamide resistant PC cells by downregulating HSP90 and AR.¹⁶

In the design of our dual AR–HDAC6 inhibitors, the intent was to maintain AR antagonist activity, while also inhibiting HDAC6. We first examined the binding mode of enzalutamide, which when compared to conventional agents like Bicalutamide, binds to the AR with higher affinity and demonstrates pure antagonist activity in preclinical models.¹⁰ After preparing the 3D structure of enzalutamide using LigPrep,¹⁷ we performed IFD to the ligand binding domain (LBD) of human AR (pdb code: 1T63)¹⁸ to understand its binding mode. The computational methods used are described in Supporting information (SI) section. Figure 1a illustrates the key interactions in 2D, highlighting the hydrophobic nature of the LBD and active site hydrogen bonds. The poses obtained from induced fit docking (IFD) shows that the trifluoromethyl group makes favorable van Der Waals (vdW) contacts with hydrophobic residues Val746, Met749, Phe764 and Leu873. Also the A ring of

enzalutamide (Fig. 1b) forms a T-shaped pi-pi stacking interaction with Phe764. The cyano group forms H-bonds with two key active site residues—Arg752 and amide of Gln711. This group occupies the same position as the keto group in the endogenous substrate dihydrotestosterone (DHT). The amide oxygen is involved in an H-bond with Asn705. We also observed that the methyl amide part of enzalutamide points towards Helix12 (Fig. 1b) of the LBD, which was crucial for our design strategy moving forward.

HDAC inhibitors typically have a zinc binding group (ZBG) which is attached to a cap group through a hydrophobic linker. Many of the reported HDAC inhibitors have an aromatic cap group such as indole (Panobinostat¹⁹) or phenyl (suberoylanilide hydroxamic acid, SAHA/Vorinostat¹⁹) groups. Until recently, no structure for HDAC6 or any other class IIb HDACs was available to guide inhibitor design. Two recent Letters detailing the structure of human and zebrafish HDAC6^{20,21} have added valuable insights to our design approach. Crystal structures of Vorinostat and Panobinostat bound to HDAC6²¹ show that the hydroxamic acid in these pan-HDAC inhibitors interacted with the active-site Zn²⁺ in a bidentate mode that was distinctly different from the HDAC6-selective inhibitor N-hydroxy-4-(2-((2-hydroxyethyl)(phenyl)amino)-2-oxoethyl)benzamide (HPOB), which had a monodentate interaction with Zn²⁺. Moreover, the cap group of these pan-HDAC inhibitors appear to make interactions with the L1 loop (D460–P484) that may favor binding to HDAC1–3. Despite having almost the same first zinc coordination shell, different hydroxamate-zinc coordination modes are observed in HDACs. For example, the zinc binding mode is bidentate in HDAC8 (PDB code 1T69) and monodentate in HDAC7 (PDB code C0Z20). The nature of this coordination appears to be strongly driven by the local environment around zinc and water in this binding channel.²² Without further detailed investigation and comparing binding energies of the ligands being investigated here (such as using high level quantum mechanical methods), it is not possible to determine if the zinc coordination mode is indeed a key player for selectivity.

With the knowledge that the methyl amide attached to the distal phenyl group of enzalutamide points towards Helix12, we proposed to use this phenyl group as the point of attachment of the HDAC inhibitor, through a suitable linker, as illustrated in Figure 2. The cyanotrifluoromethyl phenyl group (A-ring) and the thiohydantoin (B-ring) would be maintained to participate in key interactions with the AR ligand binding domain. In this design, the HDAC inhibitor is positioned such that it putatively points towards Helix12, thus maintaining AR antagonist activity. Enzalutamide would replace the aromatic cap of typical HDAC inhibitors. We planned to explore a variety of linkers as well as zinc-binding groups to accomplish our objective of dual AR–HDAC6 inhibition.

Our compound designs included a number of published Zn chelating groups (Fig. 3). These incorporated a thiophene trifluoromethyl ketone (**1**), 2-aminobenzamides (**2**, **11** and **12**), hydroxypyridones (**4**, **5**), hydroxypyridine-thione (**3**), sulfamides (**6**, **7**) and hydroxamic acids (**8**, **9**, **10**, **13** and **14**).

In order to synthesize the proposed compounds, we prepared two key intermediates **18** and **19**. The synthesis of compound **18** has been reported;²³ a similar process was used to synthesize the bromophenyl compound **19**. The routes for the synthesis of the target molecules are shown in Scheme 1. The details of the syntheses can be found in SI.

Our evaluation of the synthesized compounds began with binding assays for AR and HDAC family proteins (Table 1). To identify activity against HDAC family proteins we screened for inhibition of several Class I HDACs (HDAC1, 2, and 3) and our target, the Class IIb HDAC6 using a fluorogenic readout of de-acetylation of target peptides to quantitate de-acetylation activity.²⁴ While pan-HDAC inhibitors have shown therapeutic promise, we focused on the described synergy of HDAC6 specific inhibition with an AR

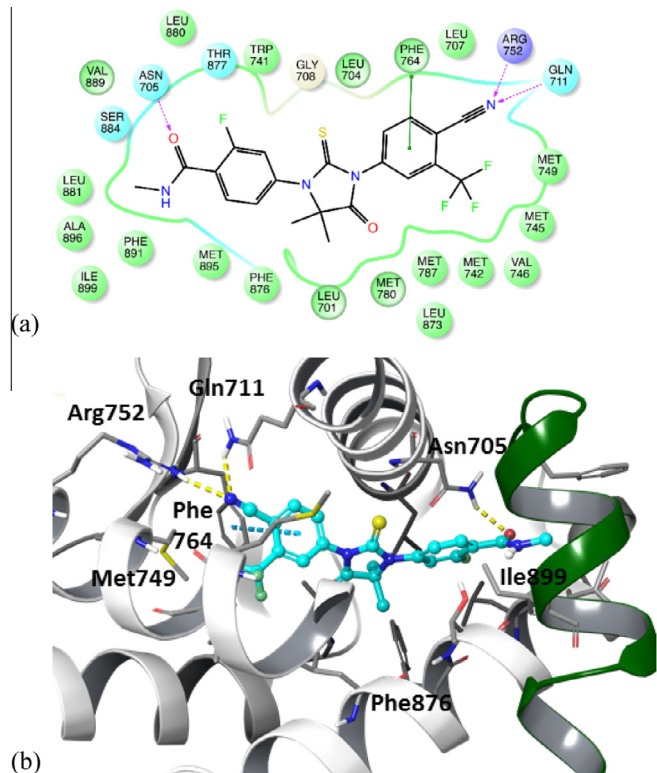


Figure 1. IFD pose of enzalutamide bound to AR. (a) Interaction of enzalutamide with AR represented in 2D. (b) The methyl amide points towards Helix12 shown in green. Enzalutamide is shown in blue ball and stick model. The key residues that interact with enzalutamide are labeled. The residues Arg752 and amide of Gln711 form H-bonds with the cyano group whereas Asn705 engages the methyl amide tail of enzalutamide. Phe764 forms a pi-pi stacking interaction with the cyanotrifluoromethyl phenyl-ring.

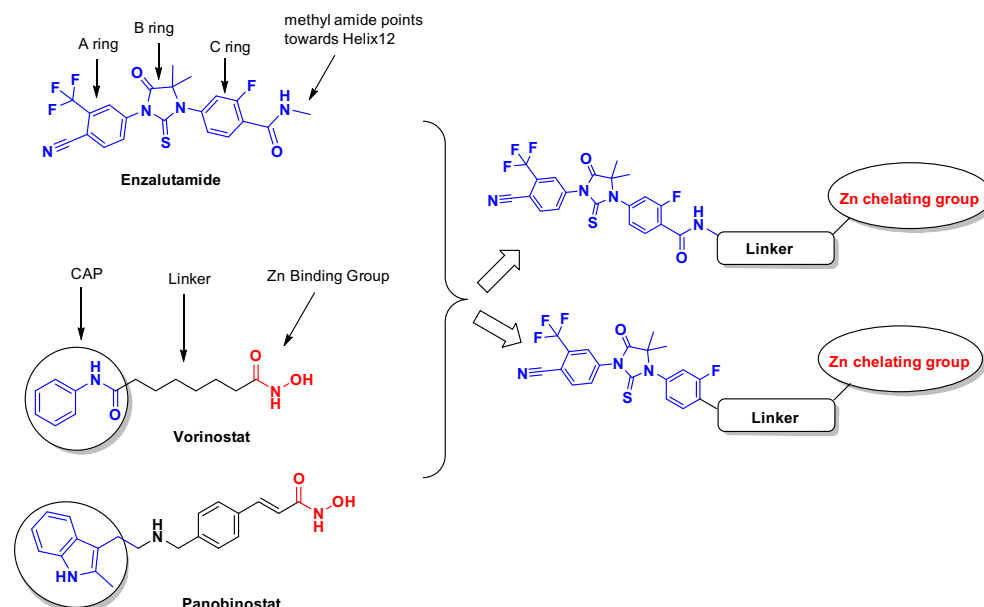


Figure 2. Compound designs incorporating enzalutamide for AR binding and a Zn-chelating group to bind HDAC.

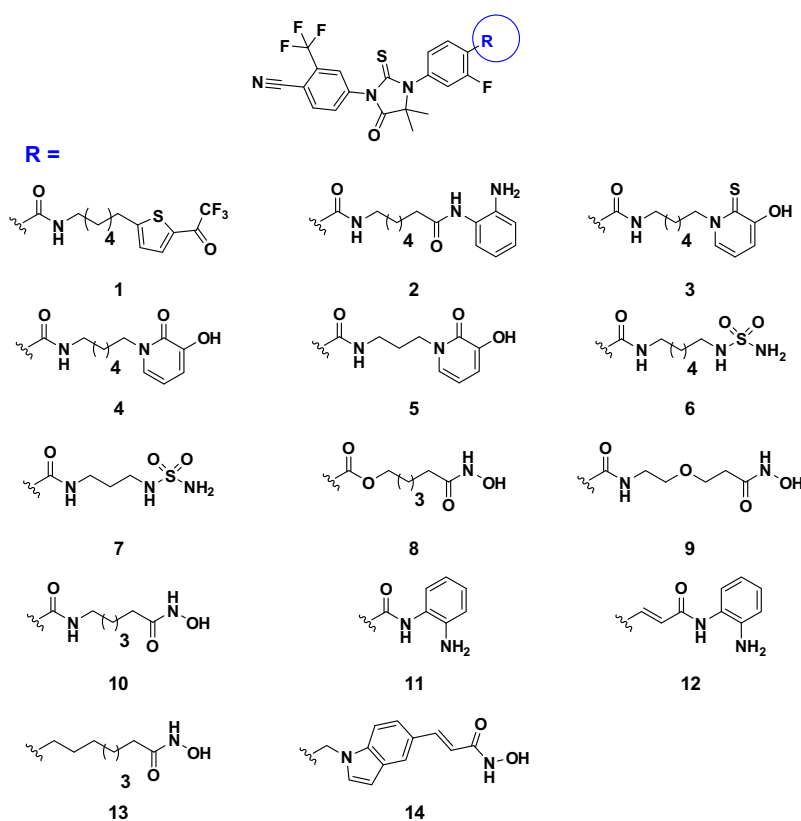
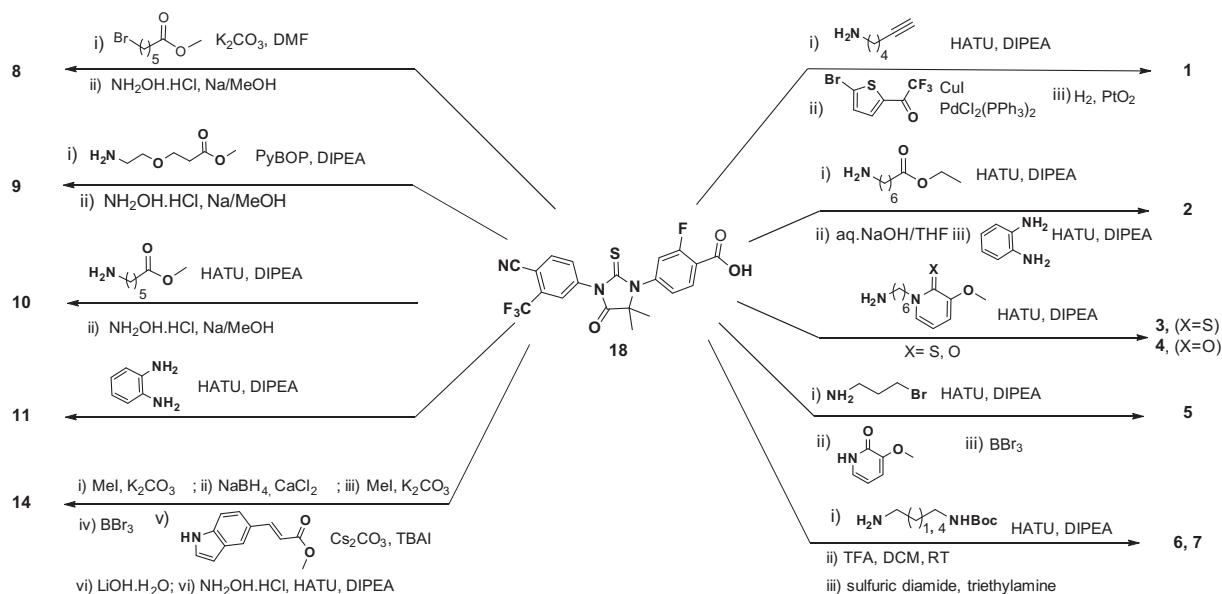


Figure 3. Structures of compounds to target AR and HDAC6.

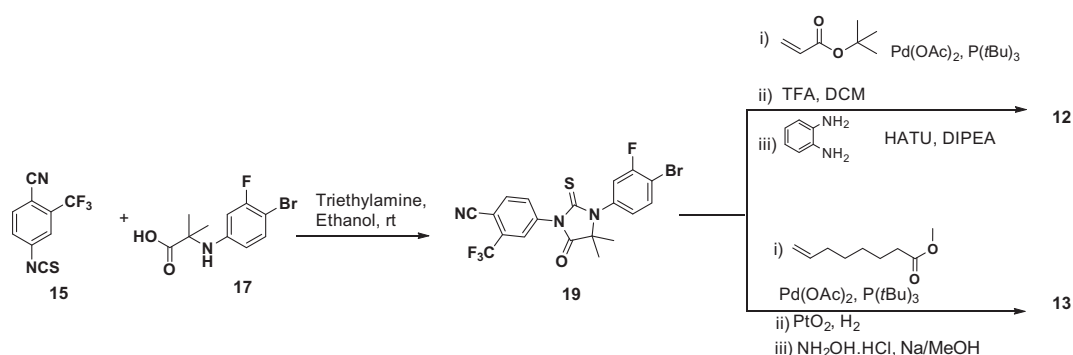
antagonist to minimize toxicity issues and maximize the therapeutic benefit. The results are listed in Table 1 with Trichostatin A used as a positive control as a pan-HDAC inhibitor. The hybrid conjugates with hydroxamic acids as zinc binding groups (compounds 8–10) showed HDAC6 specific inhibition while retaining AR antagonistic activity. Replacing the linker amide or ester in 8 and 9 with methylene groups as in 13, tends to reduce HDAC6 binding activity. Among the other zinc chelating moieties tested, the sulfamide (6) may also

provide an interesting starting point for optimization of a dual inhibitor of AR and HDAC6. Focusing on the more potent hydroxamic acid leads, we recognized that compound 8 (an ester) may not be metabolically stable *in vivo*. While it provided an interesting SAR point, we decided to follow-up on the amide analog 10 to gain further insights about the potential of such dual-acting compounds.

We tested for AR binding using a radio-ligand binding assay, where compounds were examined for the ability to inhibit



Scheme 1a. Synthesis of compounds 1–11 and 14.



Scheme 1b. Synthesis of compounds 12 and 13.

Table 1
AR and HDAC panel binding affinities

Compound ID	HDAC1 IC ₅₀ (μM)	HDAC2 IC ₅₀ (μM)	HDAC3 IC ₅₀ (μM)	HDAC6 IC ₅₀ (μM)	AR binding IC ₅₀ (μM)
1	>10	>10	>10	>10	0.068
2	>10	3.37	0.28	>10	<0.03
3	>10	3.33	>10	>10	<0.03
4	>100	>100	>100	>100	0.25
5	>100	>100	>100	14	0.56
6	>100	>100	>100	1.12	0.11
7	>100	>100	>100	>100	0.35
8	3.15	1.1	2	0.002	0.043
9	58.1	86.5	49.2	0.495	0.078
10	2.89	2.25	1.83	0.036	<0.03
11	6.19	14.1	5.4	47.3	0.33
12	>100	>100	20.2	60	0.23
13	20.6	15	10.7	0.17	<0.03
14	>100	>100	>100	2.03	<0.03
Trichostatin A	0.023	0.024	0.014	0.005	—
Enzalutamide	—	—	—	—	0.021 ¹⁰

[³H]-Mibolerone binding to AR purified from membrane fractions.²⁵ All the compounds have sub-micromolar AR binding affinity, as shown in Table 1. This was not surprising, considering our design had maintained most of the enzalutamide structure intact. Our lead HDAC6 selective compounds (8–10) also show potent AR binding affinity (Table 1). Compound 8 has a binding affinity

to AR that is comparable to that published for enzalutamide at 21 nM.¹⁰

In order to understand the binding and HDAC6 selectivity of our lead compounds, the recently determined crystal structure of HDAC6 (pdb code: 5G0J)²⁰ was used as a starting point for docking calculations. The raw X-ray coordinates for the structure of HDAC6

was subjected to additional refinement steps using the protein preparation wizard²⁶ as discussed in SI. The ligands were prepared using the LigPrep workflow with a metal binding state for the ligands. Default IFD²⁷ workflow was used for docking. Docking of compounds **8**, **9**, **10**, **13** and **14** produced reasonable binding poses where the ligand binds in a way such that the hydroxamate group is positioned correctly to 'chelate' Zn, a binding mode observed in other HDAC inhibitors (see Fig. 4). The alkyl chain linker attached to the hydroxamate group is sandwiched between a number of hydrophobic aromatic residues such as F583 and F643, which is consistent with binding similar inhibitors to other HDACs. In order to explain the SAR across this series, we estimated the ligand strain originating from varying the linker. Ligand strain calculations were carried out using Prime MM-GBSA method.^{28,29} Calculations were done on the free ligand and on the ligand bound in the geometry it adopts in the HDAC6 complex, both with implicit solvent present. The strain energy is the difference between the two energies. Qualitatively, we observe a good correlation between ligand strain and measured IC₅₀ values. For example, compound **8** (IC₅₀ = 0.002 μ M) has a ligand strain of 3.4 kcal/mol as compared to a weaker binder such as compound **13** (IC₅₀ = 0.17 μ M), which has a ligand strain of 9.6 kcal/mol. The increased ligand strain of compound **13** can be explained by the flexibility in the linker in compound **13**, compared to the amide linker of compound **8**. Based on the predicted binding mode, compound **9** (IC₅₀ = 0.5 μ M) has a hydrophilic O which may not be ideal to fit in the hydrophobic channel lined with F583 and F643, which may result in lower potency.

We proceeded to evaluate the cell-based activity of selected compounds in two key assays. First, we tested the potential AR antagonist activity by using a cell line, MDA-kb2, that stably expresses an androgen-responsive firefly luciferase reporter.³⁰ To this end, we co-incubated cells with DHT and different concentration of our hybrid molecules and we calculated how much inhibition they have when compared to a DHT only control. We also included enzalutamide as a positive control for the inhibition of this DHT-mediated AR activation. We observed a concentration dependent inhibition that was comparable to enzalutamide with our compounds (Fig. 5), suggesting that the inherent antagonist activity associated with the AR-targeted portion of the molecule remains intact. To further determine the effects of AR antagonists and differential inhibition of HDAC activity, we then tested several

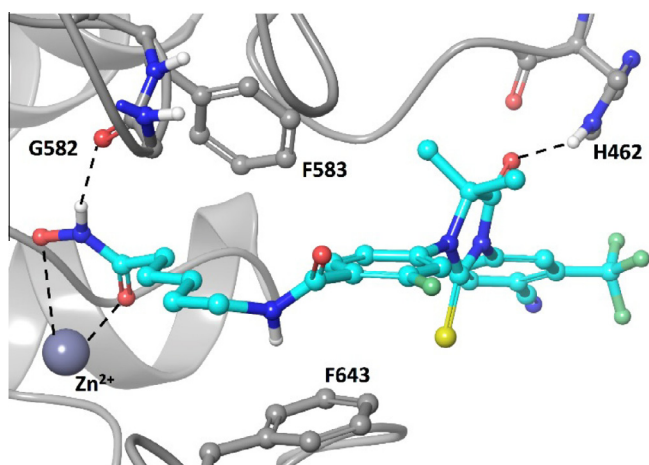


Figure 4. Glide docking of compound **10** to HDAC6 X-ray structure. The hydroxamate forms bi-dentate interaction with Zn²⁺. The linker occupies a rather hydrophobic channel lined by residues-F583 and F643. An additional H-bond with the backbone amide of G582 is seen as well. The cap region forms a hydrogen bond with H462 from the loop L1.

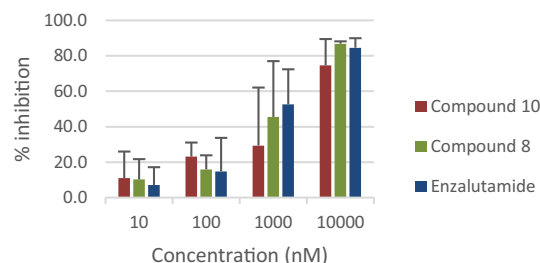


Figure 5. Cellular antagonist activity of compounds **8** and **10**, compared with enzalutamide. Compounds were tested at 10, 100, 1,000 and 10,000 nM for inhibition of DHT-stimulated AR activity in charcoal-stripped-serum (CSS) using the MDA-kb2 reporter cell line. MBD-kb2 cells were seeded at a density of 10,000 cells per well and kept in complete media for 24 h. Then, the media was replaced with media containing 5% CSS and cells were incubated for another 48 h. Cells were then treated with 10 nM DHT in presence of different concentrations of compounds **8** and **10** or the positive control enzalutamide, as noted. Relative luciferase levels were determined and normalized to vehicle-treated cells.

agents for the effects of a 24 h treatment on the LNCaP prostate cancer cell line stimulated with DHT (Fig. 6a). Treatment with enzalutamide alone did not alter AR or acetylation levels of tubulin, as expected. The benzamide HDAC-1 and -3 inhibitor MS-275³¹ did not affect AR levels, and mildly increased tubulin acetylation. The broad spectrum HDACi SAHA resulted in a lowering of AR levels, possibly due to inhibition of general transcriptional activity, and a dramatic increase in alpha-tubulin acetylation. The HDAC6 specific inhibitor, Tubastatin A,³² demonstrated a decrease in AR protein levels concomitantly with an increase in tubulin acetylation, supporting the reported AR–HDAC6 link.^{7,8}

We tested the effects of the dual AR–HDAC6 inhibitor molecules (**8** and **10**) as well and observed a reduction in the steady state AR protein level compared to the controls (Fig. 6b). Likewise, we observed hyperacetylation of tubulin compared to control, indicating that compounds **8** and **10** also have HDAC inhibitory activity in a cell-based assay. In these cell based assays the levels of AR was normalized using the ubiquitously expressed cytoskeletal protein

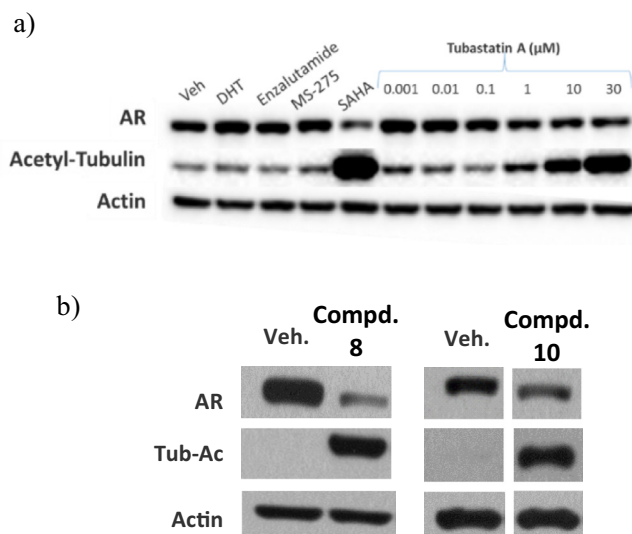


Figure 6. (a) Examination of AR and acetyl tubulin status with AR antagonist (enzalutamide, 10 μ M), Broad spectrum HDACi (MS-275, SAHA 10 μ M) or an HDAC6 specific inhibitor (Tubastatin A, doses as noted) in LNCaP cells stimulated with 10 nM DHT and indicated agents for 24 h. (b) Tubulin acetylation and AR protein levels in LNCaP cells stimulated with 10 nM DHT and treated with compounds **8** and **10** at 10 μ M for 24 h. Post treatment whole cell extracts made and resolved on an acrylamide gel. Proteins detected with antibodies against AR, acetylated tubulin and actin as a loading control. (Proteins were detected with antibodies against AR, acetylated tubulin and actin as a loading control.)

Table 2
Microsomal stability and glucuronidation potential of compound **10**

Compound #	Average human LM ^a (% rem)	Average mouse LM ^a (% rem)	Average hUGT (% rem) ^a	Average mUGT (% rem) ^a
10	29.1	21.9	97.6	46.1

^a Methods are described in [Supporting information](#).

A.

Dose Level	2 mg/kg	10 mg/kg
Route	IV	IP SC
C _{max} (μM)	0.706	0.419 0.269
T _{max} (h)	0.083	1.0 0.5
AUC _{last} (μM *h)	0.206	0.846 1.03
Terminal t _{1/2} (h)	0.427	11.0 3.42
CL (L/h/kg)	16.7	NA NA
V _z (L/kg)	10.3	NA NA
Bioavailability (%)	NA	82.1 100

B.

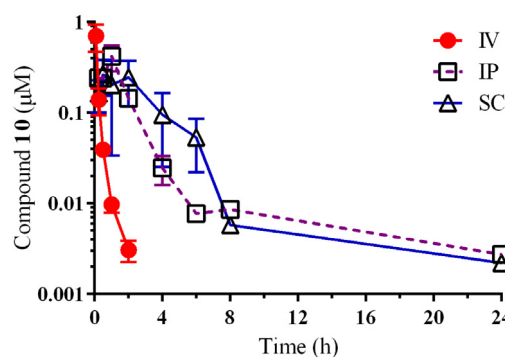


Figure 7. Pharmacokinetic evaluation of compound **10**. (A) Noncompartmental PK parameters (WinNonlin Phoenix v6.4) determined from mice ($N = 3/\text{time-point}$) in the sparse sampling mode, (B) concentration–time profiles in mice following iv (2 mg/kg), ip (10 mg/kg) or sc (10 mg/kg) administration. Methods are described in [Supporting information](#).

actin. The ability of these dual inhibitor molecules to inhibit AR signaling and to reduce the AR protein levels indicates a new approach to targeting prostate cancer that may be applicable to patients who are resistant to currently approved therapies.

With compounds that demonstrated effects on AR and HDAC6 in LNCaP cells, we began to focus on PK properties for this chemical scaffold. Lead compound **10** was evaluated for in vitro microsomal stability in both human and mouse liver microsomes (Table 2). We observed low microsomal stability in human and mouse NADPH-supplemented microsomal incubations. Furthermore, since hydroxamic acid based HDAC inhibitors are known to undergo extensive glucuronidation,³³ we tested the stability of compound **10** in the in vitro human and mouse UGT assays (Table 2). Interestingly, it showed a lower potential for glucuronidation in a human assay than in a mouse assay.

The lead compound **10** was also profiled for its pharmacokinetics in mouse (Fig. 7). Given its poor metabolic stability in mouse liver microsomes, we dosed **10** by the intraperitoneal (IP) and subcutaneous (SC) route of administration rather than an oral route.

Systemic clearance greater than hepatic blood flow was observed for compound **10** in mice which was approximately consistent with its high in vitro metabolic turnover in the mouse microsomal stability assay. Similar systemic exposure was achieved by the IP and SC routes of administration, suggesting that either route of administration would be acceptable for preclinical testing.

We have described efforts that have led to the discovery and in vitro and in vivo evaluation of compound **10**, a dual inhibitor of AR and HDAC6. The hydroxamic acid, which is key to HDAC inhibition is a known liability; such compounds are associated with poor pharmacokinetics and lack of selectivity among the HDAC isozymes.³⁴ Compound **10** may be a useful tool compound in pharmacology studies to evaluate the value of dual inhibition of AR and HDAC6. It would have to be dosed via SC or IP route to enable sufficient exposure in vivo. Recognizing the value of non-hydroxamate containing HDAC inhibitors, we will focus future efforts to develop the hit compound **6**. Compound **6** embodies a sulfamide as a Zn binding moiety, replacing the hydroxamate group. Docking of compound **6** into HDAC6 shows the sulfamide group engaging in a mono-dentate chelation of Zn, in addition to other interactions with the protein (Fig. S1 in SI). Compounds containing sulfamide have been previously shown to be active against Zn containing enzymes, such as human carbonic anhydrase II (for reference binding mode, see PDB code: 4FU5). Compound **6** is active as a dual inhibitor (HDAC6 IC₅₀ = 1 μM, AR IC₅₀ = 0.1 μM) and is selective for HDAC6 (>100 fold over the other isozymes tested), providing a good starting point for optimization to a lead compound.

Funding: This research did not receive any specific grant from funding agencies in the public, commercial or not-for-profit sectors. It was funded solely by Medivation.

Acknowledgements

The authors thank Dr. Andy Protter, Dr. Michael J. Green and Dr. Son M. Pham for careful reading of the manuscript and the Analytical and Purification group at Integral BioSciences for purification of compounds and for acquiring NMR data.

Supplementary data

Supplementary data associated with this article can be found, in the online version, at <http://dx.doi.org/10.1016/j.bmcl.2016.09.058>.

References and notes

- Ivaro, P. *Cancer Chemother. Pharmacol.* **2014**, *73*, 219.
- Tang, C.; Li, C.; Zhang, S.; Hu, Z.; Wu, J.; Dong, C.; Huang, J.; Zhou, H.-B. *J. Med. Chem.* **2015**, *58*, 4550.
- Gryder, B. E.; Akbashev, M. J.; Rood, M. K.; Raftery, E. D.; Meyers, W. M.; Dillard, P.; Khan, S.; Oyelere, A. K. *ACS Chem. Biol.* **2013**, *8*, 2550.
- West, A. C.; Johnstone, R. W. *J. Clin. Invest.* **2014**, *124*, 30.
- Falkenberg, K. J.; Johnstone, R. W. *Nat. Rev. Drug Disc.* **2014**, *13*, 673.
- Aldana-Masangkay, G. I.; Sakamoto, K. M. *J. Biomed. Biotechnol.* **2011**, *2011*, 875824.
- Ai, J.; Wang, Y.; Dar, J. A.; Liu, J.; Liu, L.; Nelson, J. B.; Wang, Z. *Mol. Endocrinol.* **2009**, *23*, 1963.
- Seidel, C.; Schneckeburger, M.; Mazumder, A.; Teiten, M.-H.; Kirsch, G.; Dicato, M.; Diederich, M. *Biochem. Pharmacol.* **2016**, *99*, 31.
- Abbas, A.; Gupta, S. *Epigenetics* **2008**, *3*, 300.
- Tran, C.; Ouk, S.; Clegg, N. J.; Chen, Y.; Watson, P. A.; Arora, V.; Wongvipat, J.; Smith-Jones, P. M.; Yoo, D.; Kwon, A.; Wasielewska, T.; Welsbie, D.; Chen, C. D.

- Higano, C. S.; Beer, T. M.; Hung, D. T.; Scher, H. I.; Jung, M. E.; Sawyers, C. L. *Science* **2009**, 324, 787.
11. Rathkopf, D.; Scher, H. I. *Cancer J.* **2013**, 19, 43.
 12. Chen, Y.; Scher, H. I. *Nat. Rev. Clin. Oncol.* **2012**, 9, 70.
 13. Rescigno, P.; Lorente, D.; Bianchini, D.; Ferraldeschi, R.; Kolinsky, M. P.; Sideris, S.; Zafeiriou, Z.; Sumanasuriya, S.; Smith, A. D.; Mehra, N.; Jayaram, A.; Perez-Lopez, R.; Mateo, J.; Parker, C.; Dearnaley, D. P.; Tunariu, N.; Reid, A.; Attard, G.; de Bono, J. S. *Eur. Urol.* **2016**.
 14. Antonarakis, E. S.; Lu, C.; Luber, B.; Wang, H.; Chen, Y.; Nakazawa, M.; Nadal, R.; Paller, C. J.; Denmeade, S. R.; Carducci, M. A.; Eisenberger, M. A.; Luo, J. *JAMA Oncol.* **2015**, 1, 582.
 15. Marrocco, D. L.; Tilley, W. D.; Bianco-Miotto, T.; Evdokiou, A.; Scher, H. I.; Rifkind, R. A.; Marks, P. A.; Richon, V. M.; Butler, L. M. *Mol. Cancer Ther.* **2007**, 6, 51.
 16. Rosati, R.; Chen, B.; Patki, M.; McFall, T.; Ou, S.; Heath, E.; Ratnam, M.; Qin, Z. *Mol. Pharmacol.* **2016**, 90, 225.
 17. Jain, R. P.; Vederas, J. C. *Bioorg. Med. Chem. Lett.* **2004**, 14, 3655.
 18. Estebanez-Perpina, E.; Moore, J. M. R.; Mar, E.; Delgado-Rodriguez, E.; Nguyen, P.; Baxter, J. D.; Buehrer, B. M.; Webb, P.; Fletterick, R. J.; Guy, R. K. *J. Biol. Chem.* **2005**, 280, 8060.
 19. Wagner, J. M.; Hackanson, B.; Lubbert, M.; Jung, M. *Clin. Epigenet.* **2010**, 1, 117.
 20. Miyake, Y.; Keusch, J. J.; Wang, L.; Saito, M.; Hess, D.; Wang, X.; Melancon, B. J.; Helquist, P.; Gut, H.; Matthias, P. *Nat. Chem. Biol.* **2016**.
 21. Hai, Y.; Christianson, D. W. *Nat. Chem. Biol.* **2016**.
 22. Wu, R.; Lu, Z.; Cao, Z.; Zhang, Y. *J. Am. Chem. Soc.* **2011**, 133, 6110.
 23. Jain, R. P.; Angelaud, R.; Thompson, A.; Lamberson, C.; Greenfield, S. *PCT Int. Appl.* **2011**.
 24. Howitz, K. T. *Drug Discovery Today Technol.* **2015**, 18, 38.
 25. Traish, A. M.; Muller, R. E.; Wotiz, H. H. *Endocrinology* **1986**, 118, 1327.
 26. Sastry, G. M.; Adzhigirey, M.; Day, T.; Annabhimoju, R.; Sherman, W. J. *Comput. Aided Mol. Des.* **2013**, 27, 221.
 27. Sherman, W.; Beard, H. S.; Farid, R. *Chem. Biol. Drug Des.* **2006**, 67, 83.
 28. Miller, E. B.; Murrett, C. S.; Zhu, K.; Zhao, S.; Goldfeld, D. A.; Bylund, J. H.; Friesner, R. A. *J. Chem. Theory Comput.* **2013**, 9, 1846.
 29. Guimaraes, C. R. W.; Cardozo, M. J. *Chem. Inf. Model.* **2008**, 48, 958.
 30. Wilson, V. S.; Bobseine, K.; Lambright, C. R.; Gray, L. E. J. *Toxicol. Sci.* **2002**, 66, 69.
 31. Saito, A.; Yamashita, T.; Mariko, Y.; Nosaka, Y.; Tsuchiya, K.; Ando, T.; Suzuki, T.; Tsuruo, T.; Nakanishi, O. *Proc. Natl. Acad. Sci. U.S.A.* **1999**, 96, 4592.
 32. Butler, K. V.; Kalin, J.; Brochier, C.; Vistoli, G.; Langley, B.; Kozikowski, A. P. *J. Am. Chem. Soc.* **2010**, 132, 10842.
 33. Kang, S. P.; Ramirez, J.; House, L.; Zhang, W.; Mirkov, S.; Liu, W.; Haverfield, E.; Ratain, M. J. *Pharmacogenet. Genomics* **2010**, 20, 638.
 34. Suzuki, T.; Miyata, N. *Curr. Med. Chem.* **2005**, 12, 2867.